The role of Ce^{4+} ions in enhancing Structure and shielding properties in cerium phosphate glasses

Fawzia Zaid **Marwa Elbishty**
fouzia_zaid@yahoo.co.uk marwaelbishty@gmail.com
Physics Department, Faculty of Education, University of Zawia, Libya.

الملخص:

تم استخدام التبريد السريع لتحضير عينات زجاجية في نظام $xC_eO_2(100-x)P_2O_5$ حيث ان x=10 ، 20، 30، 40 مول%. حددت أنماط حيود الأشعة السينية التي تم الحصول عليها أن العينات الزجاجية المحضرة أظهرت طبيعة زجاجية، ولكن عند استخدام المجهر الإلكتروني النافذ (TEM)يكشف عن وجود بلورات نانوية الحجم (جسيمات نانوية). تم حساب الخصائص الفيزيائية مثل الحجم المولي والكثافة وكثافة التعبئة والحجم الحر وكثافة تعبئة الأكسجين باستخدام الصيغ المناسبة. يزداد رقم الصلابة (H_v) للزجاج المدروس بزيادة محتوى CeO_2 . تم دراسة كميات التدريع الأساسية لتحديد مدى اختراق الإشعاع في الزجاج، مثل معامل التوهين الكتلي(μ_m) ، وطبقة نصف القيمة (HVL)، والعدد الذري الفعال (Z_{eff}) أثبتت النتائج أن عينات الزجاج المحضرة تمتلك فعالية فائقة في الحماية من أشعة جاما. ولهذا ممكن تستخدم كمواد تدريع لهذه الاشعة.

Abstract

Fast melt quenching was used to create glasses in the $xCeO_2(100-x)\ P_2O_5$ system x=10, 20, 30, 40 mol%. The obtained X-ray diffraction patterns determined that the prepared glass samples showed a glassy nature, but when using transmission electron microscopy (TEM), the presence of nano-sized crystals (nanoparticles) was revealed. The physical properties like molar volume, density, packing density, free volume and oxygen packing density were calculated using appropriate formulae. The Hardness number (H_v) of the investigated glasses increases with increasing CeO_2 content. The basic shielding quantities for determining the penetration of radiation in glass, such as mass attenuation coefficient (μ_m), half value layer (HVL) and effective atomic number (Z_{eff}) were investigated. The results proved that the prepared glass samples possess superior gamma-ray shielding effectiveness, so it can be used as a shielding material for these rays.

Keywords: prepared glasses, packing oxygen, mass attenuation coefficient, shielding parameters.

1. Introduction

Phosphate glasses possess unique and interesting optical, thermal, and electrical properties which make them candidates for a wide range of applications [1, 2]. The low chemical durability of phosphate glasses has been changed by the addition of multivalent oxides (such as Al_2O_3, PbO, ZnO, Fe_2O_3), the resulting glasses have extended applications including sealing glass, optical glass, and biocompatible and bioactive glasses, and even iron phosphate has been studied extensively for encapsulation of some radioactive wastes[3,4].

On the other hand, most rare-earth ions are stable in trivalent valence state and their characteristic optical spectra remain unaffected by the host glasses when melted under normal atmospheric condition because their electronic shell is protected from the effects of the ligand fields by the outer 5s and 5p electrons [5,6]. This study used the lighter rare earth cerium ions, which are frequently identified in both triple and quaternary valence states [7,8]. Cerium ions have the ability to exist in two possible valence states, i.e. Ce^{3+} and Ce^{4+}, the ratio of which depends on the host material as well as on the state of preparation. Exposure of many types of oxide glasses to ionizing radiation produces optical absorption bands in the visible. Cerium prevents the formation of these bands in such widely different glasses. Explanations for this effect often involve changes in the oxidation state of cerium, which can be present as Ce^{3+} or Ce^{4+} [9,10].

The half-value layer (HVL) and the mass attenuation coefficient (μ_m) are helpful concepts in the field of dosimeter and radiation physics protection. The mass attenuation coefficient, which is measured in (cm^2/g) and is used in the design of shielding materials, represents the incident photon interactions per unit mass of the matter [11,12]. This coefficient's size changes with the material's atomic number, density (ρ), and incident photon energy [13]. The radiation shielding materials are importance and agriculture, engineering and medical field. However, radiation shielding materials are based on the principle of radiation attenuation to reduce the effect of radiation, blocking or bouncing radiation particle though the shielding materials. In this work, study on glass radiation shielding materials.

2. Experimental technique

The [$xCeO_2$.(100-x) P_2O_5, (x= 10, 20, 30 and 40 mol%)] glasses were prepared by melt-quench technique. Reagent grade CeO_2 and $NH_4H_2PO_4$ crystalline powders were used as raw materials. The powders were mixed in the desired proportions and melted in porcelain crucibles at temperatures ranging from 1250˚C to 1320˚C, except the sample containing 40 mol% CeO_2, the powder was added part by part to simplify the melting process and the temperature is raised gradually to 1450 ˚C. This processes takes 2 hours form the first addition of the powder in the crucible to obtaining the final melt. The composition of each glass was X-ray diffraction to determine the vitreous states of the prepared samples. The samples were ground into a fine powder at Central Metallurgical Research and Development Institute XRD system with a Cu Kα radiation ($\lambda_{CuK\alpha}$=0.15406 nm). The 2θ angle scan is changed from 3° to 70° and the time per step of 0.4 seconds.

A popular method for evaluating morphology and obtaining more information about the size and shape of the bulk material is transmission electron microscopy, or TEM. Using a JEOL–JEM–2100 (Electron Microscope Unit, Mansoura University), TEM experiments were conducted.

Density was estimated using the Archimedes method by weighing the glass in th e air (w_a), submerging it in toluene (w_t), and then applying the well-known formula [14] ,

$$\frac{\rho}{\rho_t} = \frac{w_a}{w_a - w_t} \qquad (1)$$

(where t, toluene density = 0.866 g/cm3). The formula that links the glass sample's molar volume, molecular weight, and density of the glass sample [15] given by:

$$V_m = \frac{M_i n_i}{\rho} \qquad (2)$$

where M_i is the molecular weight for the component i, n_i its molar ratio, and ρ is the sample density. Packing density, ρ_d gives the measurement of rigidity of the oxide system [16] which may be determined by the formula,

$$p_d = \frac{1}{V_m}\sum V_i X_i \quad (3)$$

where V_i and X_i represent the packing factor and mole fraction of the composition, respectively. Packing factor [17] of any oxide D_XO_Y having D and O ions with ionic radii r_D and r_O may be estimated by:

$$V_i = \frac{4\pi}{3}(Xr_D^3 - Yr_O^3) \quad (4)$$

Estimated Free volume by equation:

$$V_f = V_m - \int X_i V_i \quad (5)$$

Oxygen packing density O_{pd} which defines the organization of oxygen atoms in the glasses [18] was calculated from the formula,

$$O_{pd} = \frac{1000\times O}{V_m} \quad (6)$$

where O refers to the number of oxygen atoms in the glass network.

The Vickers hardness (H_v) was tested using the diamond pyramid indentation method with a Micro/Macro Vickers Hardness Tester FALCON 500. After surface polishing each sample at room temperature, five indentations were made. The test load was 0.5 kg, with a 30 second indentation period.

Gamma-ray attenuation coefficients (μ_m) were obtained for the prepared glass samples using a collimated beam of γ-rays for nine energy lines emitted from 4.9 μCi Co-60, 9.5 μCi Cs-137, and 3.7 μCi Eu-152 radioactive sources. In this work, the experimental values of mass attenuation coefficient μ/ρ (g/cm^2) were compared with the theoretical values which were calculated by WinXCom program [19]. The experimental values of linear attenuation coefficient (μ) were measured using the narrow beam transmission geometry, by the following equation [20, 21]:

$$\mu = \ln(I_0/I)/X \quad (7)$$

where Io and I are the intensities of the incident and transmitted gamma ray energies, respectively, and x is the thickness of the glass sample under measurement. The values of mass attenuation coefficient (μ_m) were then obtained by:

$$\mu_m = \frac{\mu}{\rho} \quad (8)$$

The values of μ_m for each sample were calculated based on the mixture rule by the WinXCOM program (version 3.1) using the mixture rule of different elements as following [22]:

$$\mu_m = \sum_i \omega_i \left(\frac{\mu}{\rho}\right) \quad (9)$$

where μ_m and w_i: mass attenuation coefficient and fraction weight of the *i* the constituent element. ρ is the density of the glass sample.

By using the linear attenuation coefficient μ, the half value layer (HVL), which is the thickness required to reduce the transmitted intensity to one half the initial intensity, is determined by:

$$HVL = \frac{ln2}{\mu} \quad (10)$$

One popular metric for analyzing the interaction of gamma rays with a material made up of several elements is the effective atomic number (Z_{eff}) (glassy system for example). The quantity of photons absorbed by the glass sample will increase with larger Z_{eff} values, it is crucial to note [23].

3. Results and discussion

3. 1 XRD and TEM analysis.

Figure 1 shows XRD spectra of a binary cerium phosphate glasses of different CeO_2 concentrations. The spectra involve a broad halo peak characterizes the amorphous structure of the investigating glasses The relative intensity of the broad spectra decreases with the increase of CeO_2 content which may be argued to formation of some regular distributed cerium species which are distributed in the main amorphous structure of the glass. This argument is further confirmed from the morphology presented by the transmission electron microscopy (TEM), figure 2. It appears from TEM images that there is sphere particles like shape with little dimensions or sizes which ranges from 15 nm to 43 nm. Increasing CeO_2 to 40 mol% leads to increase the accumulation of the Ce ions to form layers like structure. In such a case an agglomerated spherical shape contains some

clusters of different sizes ranged from about 14 nm to 31 nm are formed. More increase in CeO_2 content (x=40 mol%) leads to the increase in the agglomeration process to became as interconnected collapses that form layers.

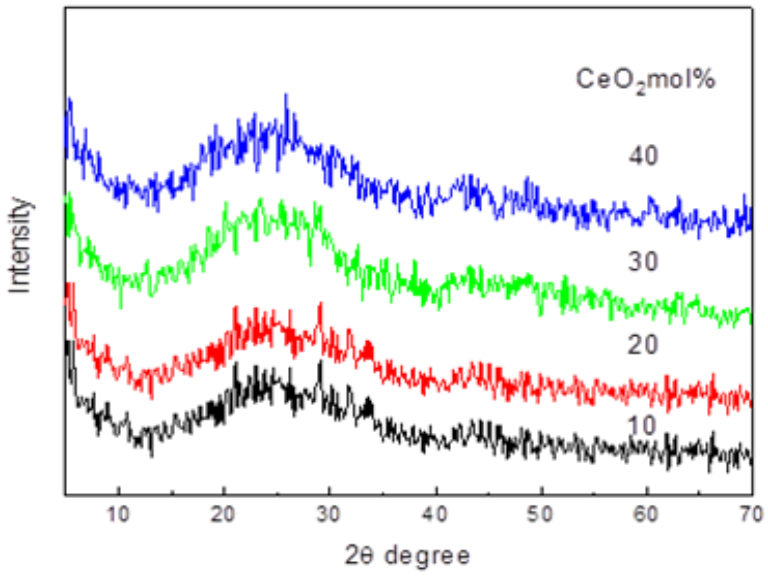

Figure. 1 XRD spectra of glasses as a function of CeO_2 concentration.

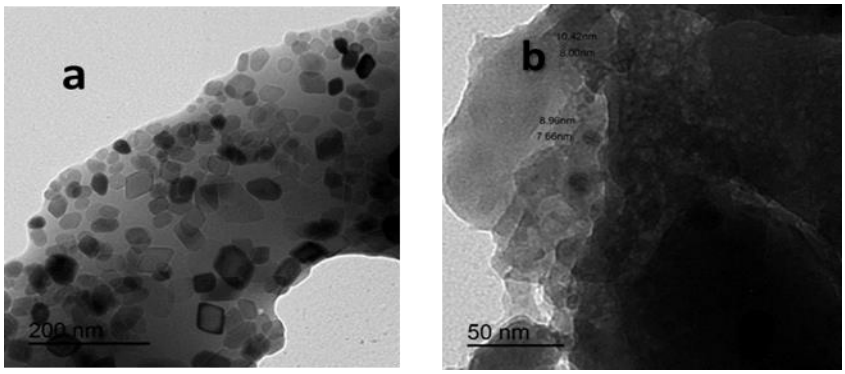

Figure 2. TEM images of the x CeO_2(100 - x) P_2O_5 glasses: **(a):** x = 10 mol %, **(b):** x= 40 mol %.

3.2 density, molar volume, Packing density and free volume.

Usually, the density of glasses directly proportional to the molecular masses [24]. In our study, the CeO_2 increased at the expense of P_2O_5 so, the density increase. The increase in density may be explained as the difference between molecular masses of P_2O_5 and CeO_2 [141.9445 & 79.866] respectively. Figure 3 shows the dependence of density (ρ) and molar volume (V_m) on the CeO_2 content in CeO_2–P_2O_5 glasses. Density of the

glass samples is found to be increasing from 2.9 to 3.8 g/cm^3 and 30.96 g/cm^3 but molar volume decreases when increasing the CeO_2 content. The molar volume of glasses directly proportional to the atomic radii and bond length of cations. In our study, the molar volume decreased, this behavior is associated with the difference of atomic radii and bond length of cerium and phosphorus cations. Atomic radii and bond length of these cations are [Ce (0.181 nm) & P (0.221 nm)] and [Ce (1.81 Å) & P (0.1 nm)] respectively. The changes in density and molar volume at these concentrations are to be attributed to changes in the glass structure. This can be confirmed by the results TEM as an increase in clusters means an increase in the formation of bridging oxygen units.

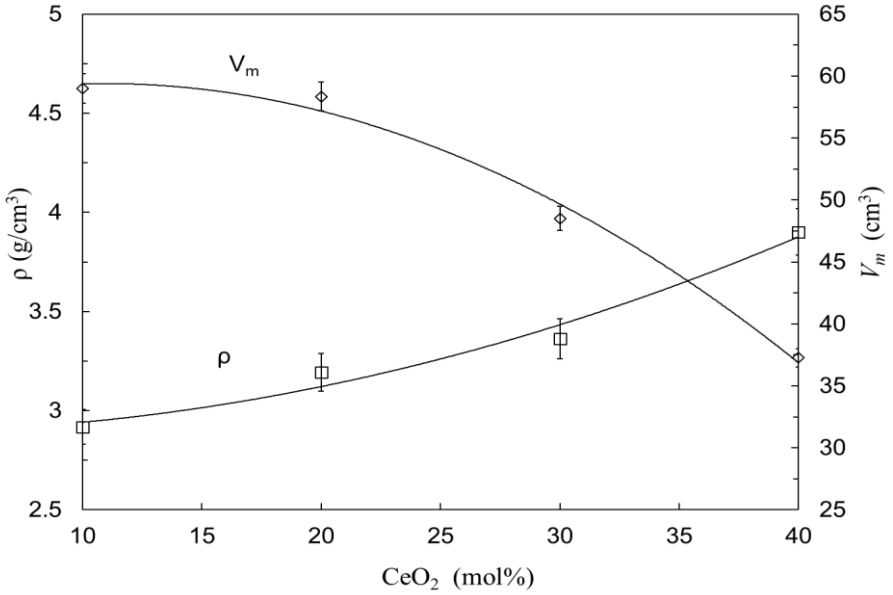

Figure 3: Variation of the experimental density and molar volume of $xCeO_2$-(100-x) P_2O_5, where \ CeO_2 = 10, 20, 30 and 40mol %.

The figure 4. shows the CeO_2 content dependence of both free volume (V_f) and packing density (P_d) in $xCeO_2(100–x)$ P_2O_5 glasses. It is observed that V_f rises slightly up to 20 mol% CeO_2 and then decreases sharply up to 40 mol% CeO_2 content. This indicates that the added intermediate oxide (CeO_2) at a rate of up to 20 mol% causes the formation of non-bridging oxygen ions (NBOs) in the phosphate matrix more than the formation of bridging Oxygen ions (BO) because this oxide is an intermediate oxide, while (CeO_2) up to 40 mol% causes in a composition of bridging Oxygen(BO) ions in the phosphate matrix [25].

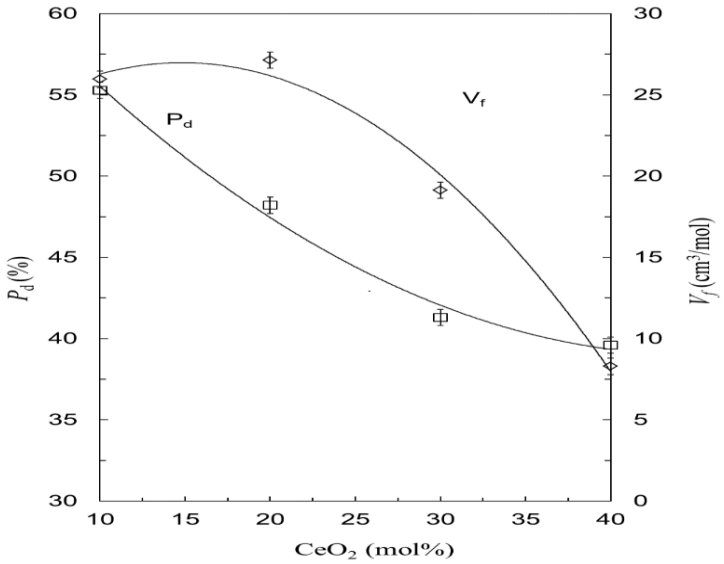

Figure 4: Variation of packing density and volume free with CeO_2. .

3.3 oxygen packing density and hardness

The behavior of oxygen packing density with increasing concentration of CeO_2 is shown in Figure 5. It was observed that there was a decrease in O_{Pd} at 20 mol% CeO_2 concentration, which is due to the generation of more non-bridged oxygen, while there was a noticeable increase in O_{Pd} when the concentration of CeO_2 increased above 20 mol%, because cerium oxide formed bonds with phosphate units, which is due to the generation of more bridging oxygen as Ce-P-Ce or P-Ce-P and the changes that have occurred in bonds.

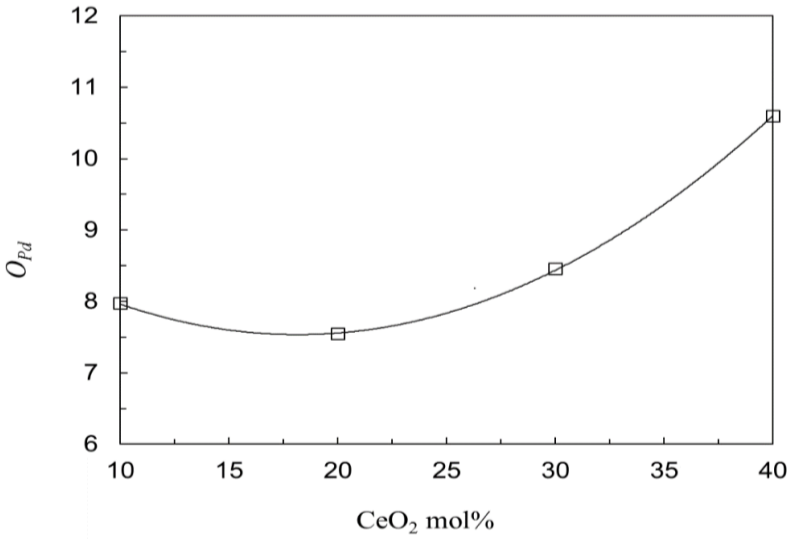

Figure. 5: Variation of Opd with CeO_2.

The dependence of "Vickers micro hardness H_v" on the CeO_2 content is seen in figure.6. Glass hardness increases linearly with increasing cerium oxide concentration, and there is a significant increase in hardness values from about 350–550.5 kg/mm^2 as cerium oxide content increases from 10 to 40 mo%. The increase in the hardness number is related to the increase in the rigidity of bulky glass. These findings are consistent with density findings, which showed that the addition of CeO_2 strengthened the network by replacing the weaker hydrated P–O–P and non-bridging oxygen bonds with the more resistant P–O–Ce or Ce–O–Ce bonds. This is confirmed by TEM and X-ray results as well [25].

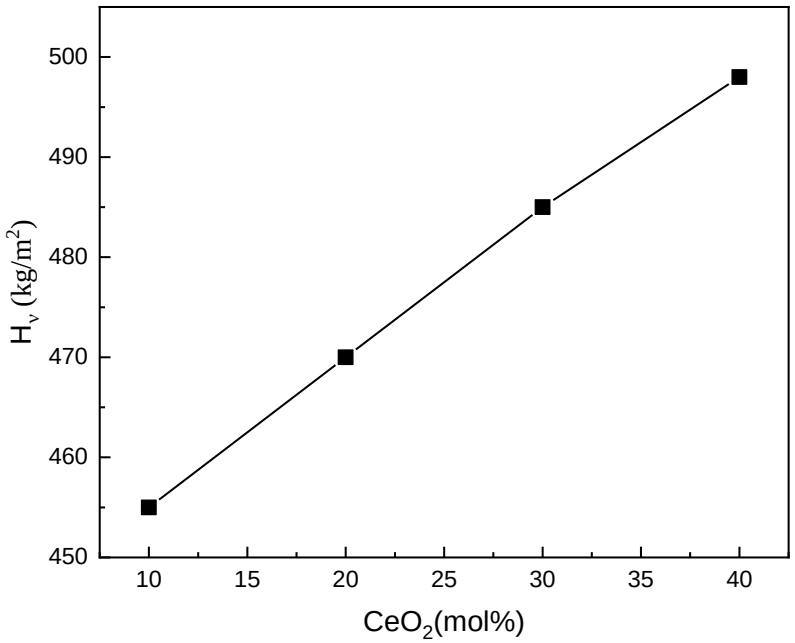

Figure.6: Micro hardness of $xCeO_2$-(100-x) P_2O_5 where x=10, 20, 30 and 40 mol %.

3.4 Gamma-rays shielding

The attenuation coefficients of gamma rays in existing glass barriers up to 3 cm thick were studied using gamma rays with the energy range 0.015-15 MeV [19]. The attenuation coefficients of the prepared glasses are checked to ensure the ability of these glasses to act as shields from harmful radiation. The linear attenuation coefficient is a factor that evaluates the ability of a material to protect when exposed to radiation. Obviously it depends on the density of the prepared glasses. The variety of μ_m versus the gamma-ray energies as a function of CeO_2 was illustrated in Figuer.6. The photon energy affects the interactions between gamma rays and the material in three ways: Compton scattering, photoelectric absorption, and pair creation. As the energy grows, the value of

μ_m drops, indicating that the manufactured glasses' shielding effectiveness decreased as photon energy grew. At the low energy region, there appears to be a rapid mass drop (attributed mostly to photoelectric absorption). It suggests that the low region's energy is what determines this parameter. At intermediate energies, however, Compton scattering predominates as an interaction. The highest frequency of pair creation occurs at very high photon energies above 1.022 MeV. [26]. The μ_m trend seen in these figures is similar to previous work on various glass systems (e.g., lead glasses) [27], and bismuth borate glasses [28].

However, in contrast, the HVL values of the studied $CeO_2$and P_2O_5 based glass systems have been estimated to evaluate the photon attenuation characteristics directly [29]. It is well-known that the smaller HVL values are the better the glass system considered is, for gamma ray's radiation shielding applications. HVL results of the present glass samples for the energy range in this study are illustrated in figure. 7. It was evident that the HVL was decreased when the CeO_2 content was increased. This behavior may result from an increase of the μ_m values and prepared glasses' density.

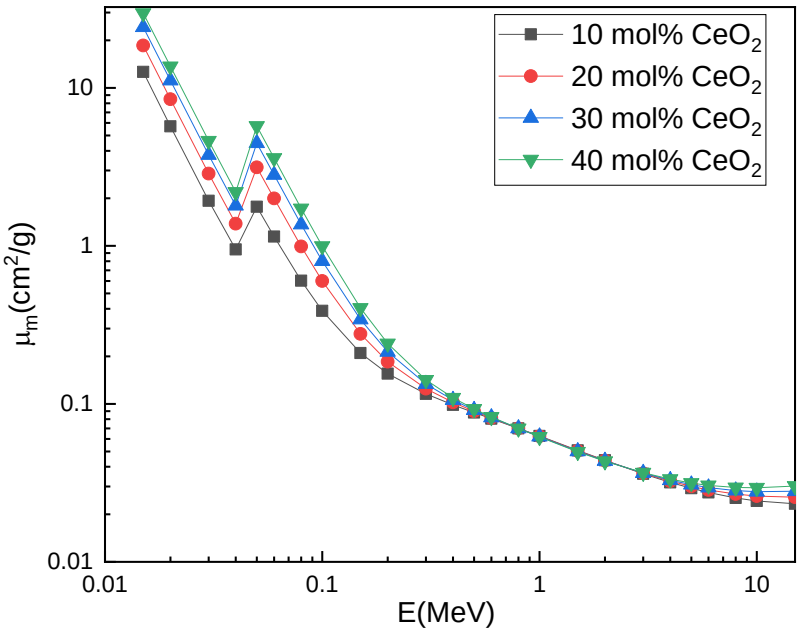

Figure 7: Mass attenuation coefficients of prepared glass system in the energy ranges from 0.015–

15 MeV and x = 10, 20, 30, 40% mol CeO_2.

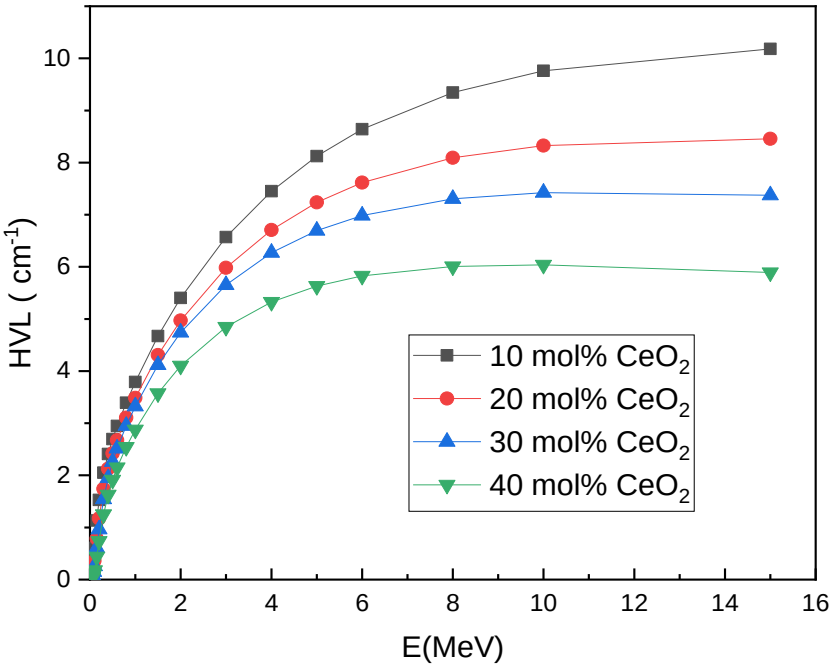

Figure. 8: HVL results of prepared glass system.

It is known that larger Z_{eff} values are necessary to obtain a better shielding material from ionization radiation because they increase the probability of photons interacting with the target. For technical, engineering and material purposes, the Z_{eff} value for composite materials is a useful parameter [30, 31]. Z_{eff} can be represented as a number that presents several properties of a material. Therefore, calculating Zev is crucial in the radiation shielding studied. The observed increase in Z_{eff} with increasing cerium concentration can be attributed to the higher atomic number of cerium compared to phosphate shown in figure 9. While the change in Z_{eff} for the prepared glassy compound in the studied energy range 0.015-15 MeV can be explained based on the probability of gamma radiation interaction at each energy photon. That being so, the energy dependence of Z_{eff} provides the same trend as previously discussed for μ_m [32]. At low energy range, photoelectric reaction dominates. As the incident photon energy increases, photo electric interaction probability will decrease, and therefore, Z_{eff} will also decrease. At the intermediate energy range, Compton interaction dominates. As the incident photon energy increases, Compton interaction probability will decrease and therefore, Z_{eff} will also decrease. At the higher energy range, more than 0.3 MeV pair production interaction dominated.

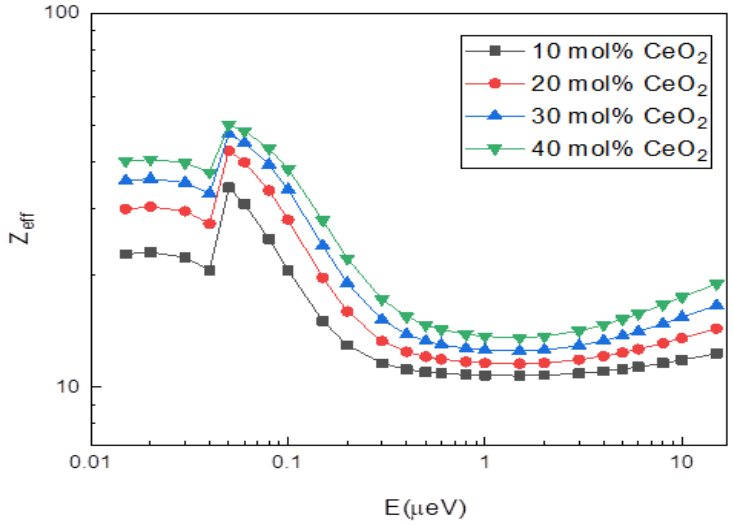

Figure 9. Effective atomic number (Z_{eff}) of the investigated glass system.

Conclusion

Structural and gamma attenuation coefficients were determined. Samples of P_2O_5 glasses with addition of CeO_2 were taken and synthesized by a simple and conservative melt-quenching method. The non-crystalline nature of the glasses was prepared and confirmed by the XRD patterns obtained but TEM spectroscopy shows nanoparticles. As the cerium oxide concentration, density increased, the molar volume, packing density, free volume and oxygen packing density decreased. This indicates that cerium ions play an unusual role in the treatment of the P_2O_5 matrix. From those of cerium Phosphate glasses. glass system was fabricated in sample thicknesses able to be applied for a lot of application as gamma radiation shielding material. The results of study of the gamma radiation shielding parameters for this glass system led to the improvement of mass attenuation coefficient (μ_m) Half Value Layer (HVL) and effective atomic number (Z_{eff}) by increasing CeO_2 concentration up to 40%, which were in a good agreement with theoretical calculation by WinXcom program. The CeO_2 glass will open new possibility for a lead free radiation protecting glass with non-toxicity to the environment. The data obtained in this study should be helpful in potential applications in gamma ray shielding materials. Finally, these glasses. It has the advantage of being transparent to visible light. It's inside particularly useful for the various shielding purposes that are offered. From favorable gamma ray sources.

References

[1] Brow, R.K., 2000. The structure of simple phosphate glasses. Journal of Non-Crystalline Solids, 263, pp.1-28.

[2] Le Saout, G., Simon, P., Fayon, F., Blin, A. and Vaills, Y., 2002. Raman and infrared study of (PbO) x (P_2O_5)(1− x) glasses. Journal of Raman Spectroscopy, 33(9), pp.740-746

[3] Hammam, M., Kilany, E., Nabhan, E., Said, A. and Atta, A., 2022. Physical, optical and radiation shielding properties of some phosphate glasses. *Egyptian Journal of Chemistry*, *65*(8), pp.499-509

[4] Mazzoni, E., Iaquinta, M.R., Lanzillotti, C., Mazziotta, C., Maritati, M., Montesi, M., Sprio, S., Tampieri, A., Tognon, M. and Martini, F., 2021. Bioactive materials for soft tissue repair. *Frontiers in bioengineering and biotechnology*, *9*, p.613787.

[5] ElBaz, N., El-Damrawi, G. and Abdelghany, A.M., 2021. Structural Role of CeO_2 in the Modified Borate Glass-Ceramics. *New Journal of Glass and Ceramics*, *11*(01), p.34.

[6] Cha, J.M., Kim, J.H. and Ryu, B.K., 2019. Effects of melting conditions on cerium oxidation state and catalytic properties of CeO_2–P_2O_5 glass systems. *Journal of nanoscience and nanotechnology*, *19*(3), pp.1829-1835.

[7] Kim, J.H., Kim, D.S. and Ryu, B.K., 2017. Effects of Melting Conditions on Cerium oxidation state and Catalytic Behavior on Cerium Phosphate Glasses. *Korean Journal of Metals and Materials*, *55*(2), pp.144-149.

[8] Shinozaki, H., Nakashima, S., Takahashi, S., Hanada, A. and Yamamoto, Y., 2013. Water resistance of cerium phosphate glasses as studied by in situ high temperature IR microspectroscopy. *Journal of non-crystalline solids*, *378*, pp.55-60

[9] Gupta, G., Chen, T.Y., Rautiyal, P., Williams, A.G., Johnson, J.A., Johnson, C.E., Edge, R. and Bingham, P.A., 2022. Antimony-modified soda-lime-silica glass: towards low-cost radiation-resistant materials. *Journal of Non-Crystalline Solids*, *585*, p.121526.

[10] Hussein, E.A. and Rammah, Y.S., 2024. Optical UV–visible, Raman spectroscopy, and gamma radiation shielding properties of borate glass systems; B_2O^{3+} Na_2O^{+} Al_2O_3/MgO/Li_2O. *Optical and Quantum Electronics*, *56*(3), p.387

[11] Alzahrani, J.S., Alothman, M.A., Eke, C., Al-Ghamdi, H., Aloraini, D.A. and Al-Buriahi, M.S., 2021. Simulating the radiation shielding properties of TeO_2–Na_2O–TiO glass system using PHITS Monte Carlo code. *Computational Materials Science*, *196*, p.110566.

[12] Kebaili, I., Znaidia, S., Alzahrani, J.S., Alothman, M.A., Boukhris, I., Olarinoye, I.O., Mutuwong, C. and Al-Buriahi, M.S., 2021. Ge20Se80-x Bi x (x≤ 12) chalcogenide glasses for infrared and gamma sensing applications: structural, optical and gamma attenuation aspects. *Journal of Materials Science: Materials in Electronics*, *32*(11), pp.15509-15522.

[13] Jackson, D.F. and Hawkes, D.J., 1981. X-ray attenuation coefficients of elements and mixtures. *Physics Reports*, *70*(3), pp.169-233.

[14] Nabhan, E., Nabhan, A., & Abd El Aal, N. (2016). Mechanical and Structural Properties of Zinc–Sodium-Phosphate Glasses Doped with Cu_2O. American Journal of Physics and Applications, 4(6), 145-151.

[15] Nurul Ain, A.M., Sahar, M.R., Sazali, E.S., Azman, K. and Yahya, N., 2017. Study on optical absorption and structural bonding of lithium zinc phosphate glasses. *Solid State Phenomena*, *268*, pp.54-61.

[16] Gowda, V.V., 2013. Effect of Bi^{3+} ions on physical, thermal, spectroscopic and optical properties of Nd^{3+} doped sodium diborate glasses. *Physica B: Condensed Matter*, *426*, pp.58-64.

[17] Inaba, S., Fujino, S. and Morinaga, K., 1999. Young's modulus and compositional parameters of oxide glasses. *Journal of the American Ceramic Society*, *82*(12), pp.3501-3507.

[18] Algradee, M.A., Alwany, A.E.B., Sultan, M., Elgoshimy, M. and Almoraisy, Q., 2017. Physical and optical properties for Nd_2O_3 doped lithium-zinc-phosphate glasses. *Optik*, *142*, pp.13-22.

[19] L. Gerward, N. Guilbert, K.B. Jensen, H.,2004. Leving,WinXCom–a program for calculating X-ray attenuation coefficients. Radiat. Phys. Chem. 71, pp. 653–654.

[20] Lamarsh, J.R. and Baratta, A.J., 2001. *Introduction to nuclear engineering* (Vol. 3, p. 783). Upper Saddle River, NJ: Prentice hall.

[21] Kumar, A., Singh, S.P., Elmahroug, Y., Kara, U., Tekin, H.O. and Sayyed, M.I., 2018. Gamma ray shielding studies on 26.66 B_2O_3–16GeO_2–4Bi_2O_3–(53.33–x) PbO–xPbF_2 glass system using MCNPX, Geant4 and XCOM. *Materials Research Express*, *5*(9), p.095203.

[22] Hubbell, J.H., 1982. Photon mass attenuation and energy-absorption coefficients. *The International Journal of Applied Radiation and Isotopes*, *33*(11), pp.1269-1290.

[23] Shamshad, L., Rooh, G., Limkitjaroenporn, P., Srisittipokakun, N., Chaiphaksa, W., Kim, H.J. and Kaewkhao, J., 2017. A comparative study of gadolinium based oxide and oxyfluoride glasses as low energy radiation shielding materials. *Progress in Nuclear Energy*, *97*, pp.53-59.

[24] Vijayakumar, M., Suriyamurthy, N., Alqahtani, M.S. and Marimuthu, K., 2024. Investigations of substantial effect on physical, structural, optical and radiation shielding properties of nitrates integrated alkaline oxyfluro phospho-silicate glasses. *Progress in Nuclear Energy*, *175*, p.105330.

[25] G. El-Damrawi, F. Gharghar, R. Ramadan, 2018. More Insight on Structure of New Binary Cerium Borate Glasses, New Journal of Glass and Ceramics 8, 12-21.

[26] Sayyed, M.I., AlZaatreh, M.Y., Matori, K.A., Sidek, H.A.A. and Zaid, M.H.M., 2018. Comprehensive study on estimation of gamma-ray exposure buildup factors for smart polymers as a potent application in nuclear industries. *Results in Physics*, *9*, pp.585-592.

[27] Hammam, M., Kilany, E., Nabhan, E., Said, A. and Atta, A., 2022. Physical, optical and radiation shielding properties of some phosphate glasses. *Egyptian Journal of Chemistry*, *65*(8), pp.499-509.

[28] El-Ghany, S.A., Nabhan, E. and Saudi, H.A., 2020. Effect of gamma ray on some properties of bismuth borate glasses containing different transition metals. *SN Applied Sciences*, *2*, pp.1-11.

[29] Akman, F., Kaçal, M.R., Sayyed, M.I. and Karataş, H.A., 2019. Study of gamma radiation attenuation properties of some selected ternary alloys. *Journal of Alloys and Compounds*, *782*, pp.315-322.

[30] Kurudirek, M., Chutithanapanon, N., Laopaiboon, R., Yenchai, C. and Bootjomchai, C., 2018. Effect of $Bi_2O=$ on gamma ray shielding and structural properties of borosilicate glasses recycled from high pressure sodium lamp glass. *Journal of Alloys and Compounds*, *745*, pp.355-364.

[31] Wilson, M., 2019. Optimization of the radiation shielding capabilities of bismuth-borate glasses using the genetic algorithm. *Materials Chemistry and Physics*, *224*, pp.238-245.

[32] Al-Buriahi, M.S., Bakhsh, E.M., Tonguc, B. and Khan, S.B., 2020. Mechanical and radiation shielding properties of tellurite glasses doped with ZnO and NiO. *Ceramics International*, *46*(11), pp.19078-19083.